3.3 Strongly Correlated Quantum Systems

Mechanism of pseudogap and superconductivity with low-energy fermionic excitations in high-T_c cuprates

Masatoshi IMADA

Department of Applied Physics, The University of Tokyo,

Hongo 7-3-1, Bunkyo-ku, Tokyo 113-8656

Recent progress in accuracy of numerical simulations has enabled much more precise determination of the ground states of the strongly correlated systems than before. Thanks to the progress, it has recently been elucidated how the *d*-wave superconducting and stripe states are severely competing in the simple Hubbard models by using combined variational Monte Carlo, tensor network and Lanczos methods [1,2] consistently with other methods. It has revealed that the ground states of most part of carrier doped Mott insulator in the Hubbard model are various periodicity of stripe states.

On the other hand, *ab initio* Hamiltonian of carrier doped $HgBa_2CuO_4$ recently derived without any adjustable parameters beyond model studies [3,4] by applying multi-scale *ab initio* scheme for correlated electrons (MACE) has been studied by applying the same improved numerical method [5], where the competition of stripe and superconductivity well reproduces the experimental phase diagram. More concretely, a high-T_c cuprate superconductor $HgBa_2CuO_{4+}$ has been studied by solving an *ab initio* low-energy effective Hamiltonian. Its ground-state phase diagram reproduces experiments including Mott gap, antiferromagnetic ordered moment in the mother material and superconducting phase extended in a wide range of hole density, which severely competes with a period-4 charge ordered state near $\delta \sim 0.1$ as is observed by recent X-ray scattering measurements. Crucial role of off-site interactions on the amplitude and stability of the superconductivity is revealed. Furthermore, we find that the enhancement of superconductivity is well correlated with that of charge fluctuations rather than spin fluctuations.

Based on the superconductivity reproduced by the numerics, we have also studied the superconducting mechanism in more depth. An experimental long-standing puzzle was the featureless structure in the spectral function indicated by the angle resolved photoemission spectroscopy (ARPES) spectra, in contrast to the case of conventional strong-coupling BCS superconductors in the history. We have shown before how the puzzle has been solved with the help of quantum-cluster studies of dynamical mean-field theory (DMFT) of the Hubbard model, where the featureless structure is a consequence of the cancellation of the prominent peaks in both of the normal anomalous part of self-energies [6,7].

We have recently examined this problem from a completely independent machine learning studies purely based on the ARPES data [8]. Recent progress of machine-learning techniques opens possibilities of exposing physical quantities hidden in direct measurements only from available experimental data combined with nonlinear regression analyses. The Boltzmann-machine method has been applied to the angle-resolved photoemission spectroscopy spectra of cuprate superconductors. The result shows that prominent peak structures exist both in normal and anomalous self-energies, but they cancel in the total self-energy making the structure apparently invisible, while the peaks make dominant contributions to superconducting gap, hence providing a decisive testimony for the origin of superconductivity. This is consistent with the former DMFT studies of the Hubbard model. The present achievement opens avenues for innovative machine-learning spectroscopy method. An emergent dark fermion theory has also been discussed in detail in connection to the peak structure revealed above [9].

We have further formulated a method of deriving effective low-energy Hamiltonian for nonperiodic systems such as interfaces for strongly correlated electron systems by extending MACE to make challenging studies of lattice relaxation around the interface possible. We have applied the formalism to copper-oxide high T_c superconductors in an example of the interface between overdoped $La_{2-x}Sr_xCuO_4$ and Mott insulating La_2CuO_4 recently realized experimentally [10]. We show that the parameters of the two-orbital *Eg* Hamiltonian derived for the $La_2CuO_4/La_{1:55}Sr_{0:45}CuO_4$ superlattice differ considerably from those for the bulk La_2CuO_4, particularly significant in the partially-screened Coulomb parameters and the level difference between the d_{x2-y2} and d_{z2} orbitals, ΔE. Here, the lattice relaxation on the E_g Hamiltonian has been examined from first principles. We find that the CuO_6 octahedra distort after the relaxation as a consequence of the Madelung potential difference between the insulator and metal sides, by which the layer dependence of the hopping and Coulomb parameters becomes more gradual than the unrelaxed case. Furthermore, the structure relaxation dramatically changes the ΔE value and the occupation number at the interface. This study not only evidences the importance of the ionic relaxation around interfaces but also provides a set of layer-dependent parameters of the *ab initio Eg* Hamiltonian, which is expected to provide further insight into the interfacial superconductivity when solved with low-energy solvers.

This is a combined report for E project “Mechanism of pseudogap and superconductivity with low-energy fermionic excitations in high-T_c cuprates”, D project “Highly accurate analysis of an effective Hamiltonian for high-T_c cuprates by the many-variable variational Monte Carlo method combined with tensor network”, and shared project for post-K project “Applications of highly accurate lattice model solvers with

tensor network and machine learning for mechanisms of superconductivity".
and "Emergent phenomena from combined strong electron correlation and electron-Phonon coupling"

This series of work has been done in collaboration with M. Hirayama, T. Ohgoe, K. Ido, A.S. Darmawan, Y. Nomura, Y. Yamaji, T. Misawa, T. Tadano, T. J. Suzuki, T. Yoshida, A. Fujimori, S. Sakai, and M. Civelli,. The calculations were performed on computers at the Supercomputer Center, ISSP, Univ. of Tokyo. The work is also supported by JSPS Kakenhi 16H06345, the RIKEN Center for Computational Science under the HPCI project (hp170263 and hp180170) and the MEXT HPCI Strategic Programs, CDMSI. This project has used the software HPhi and mVMC.

References

[1] Kota Ido, Takahiro Ohgoe, and Masatoshi Imada, Phys. Rev. B. **97**, 045138 (2018).

[2] Andrew S. Darmawan, Yusuke Nomura, Youhei Yamaji, and Masatoshi Imada, Phys. Rev. B **98**, 205132 (2018).

[3] Motoaki Hirayama, Youhei Yamaji, Takahiro Misawa, and Masatoshi Imada, Phys. Rev. B **98**, 134501 (2018).

[4] Motoaki Hirayama, Takahiro Misawa, Takahiro Ohgoe, Youhei Yamaji, and Masatoshi Imada, arXiv:1901.00763.

[5] Takahiro Ohgoe, Motoaki Hirayama, Takahiro Misawa, Kota Ido, Youhei Yamaji, and Masatoshi Imada, arXiv:1902.00122.

[6] Shiro Sakai, Marcello Civelli, and Masatoshi Imada, Phys. Rev. Lett. **116**, 057003 (2016).

[7] Shiro Sakai, Marcello Civelli, and Masatoshi Imada, Phys. Rev. B. **94**, 115130 (2016).

[8] Youhei Yamaji, Teppei Yoshida, Atsushi Fujimori, Masatoshi Imada, arXiv:1903.08060.

[9] Masatoshi Imada and Takafumi J. Suzuki, J. Phys. Soc. Jpn. **88**, 024701 (2019).

[10] Terumasa Tadano, Yusuke Nomura, Masatoshi Imada, arXiv:1902.03743.

Study on frustrated quantum spin systems using machine-learning solvers

Yusuke NOMURA and Masatoshi IMADA

Department of Applied Physics

The University of Tokyo, Hongo, 7-3-1, Bunkyo-ku, Tokyo 113-8656

Frustrated spin systems may host spin liquid ground states. Once the spin liquid states are realized, we can expect several intriguing behaviors such as fractionalized excitation. Therefore, possibility of realizing spin liquid states is investigated intensively from both experiment and theory.

One of the candidate Hamiltonians for realizing spin liquid is J_1-J_2 Heisenberg model on the two-dimensional square lattice, where the next nearest neighbor exchange J_2 competes with the nearest neighbor exchange J_1, with geometrical frustration. Despite much numerical effort, the controversy on the ground state of the square-lattice J_1-J_2 Heisenberg model has not been settled yet.

In the present study, we introduce very accurate variational wave functions utilizing machine learning techniques to investigate the ground state of J_1-J_2 Heisenberg model. The variational wave function is constructed by combining the restricted Boltzmann machine (RBM) and the pair-product (PP) states. The RBM is a type of artificial neural networks, allowing for a flexible and unbiased description of a wide variety of quantum states [1]. The PP wave function or geminal wave function used in conventional wave-function methods properly describes nonlocal entanglement, helping machine learning to learn many-body ground states efficiently. The combined wave function has been shown to give highly accurate results [2].

Using the accurate RBM+PP wave function, we investigate the possible spin liquid in the J_1-J_2 Heisenberg model. In particular, we focus on the correlation ratio and level crossing. The correlation ratio is based on the ratio between the peak value of structure factor in the momentum space and the value at the neighboring momentum, and is a very sensitive probe for the phase transition [3]. The level crossing of the excited states is also useful in detecting the phase transition [4]. Our numerical results of the correlation ratio and level crossing both suggest a spin liquid ground state for a finite range of J_2 around $J_2/J_1 = 0.5$. The spin liquid in this model is shown to be gapless, in which both the singlet and triplet sectors become gapless.

References

[1] G. Carleo and M. Troyer, Science **355**, 602

(2017).

[2] Y. Nomura, A. S. Darmawan, Y. Yamaji, and M. Imada, Phys. Rev. B **96**, 205152 (2017).

[3] R. K. Kaul, Phys. Rev. Lett. **115**, 157202 (2015).

[4] L. Wang and A. W. Sandvik, Phys. Rev. Lett. **121**, 107202 (2018).

Theoretical and numerical study on novel quantum phenomena in spin-orbit coupled materials

Yukitoshi MOTOME

Department of Applied Physics,

The University of Tokyo, Bunkyo, Tokyo 113-8656

We have theoretically studied a variety of intriguing phenomena in correlated electron systems with strong spin-orbit coupling. During this fiscal year, we have been making substantial progress on the following topics (project numbers: H30-Ca-0064 and H30-Cb-0014). We have also devoted our efforts to a closely related topic on the Kitaev-type quantum spin liquids (project number: H30-D-0005). We summarize the main achievements for each topic below.

(i) *Magnetielectric effect*: We have performed a systematic study of the magnetic phase diagrams and magnetoelectric responses for a simple model that we constructed for a family of compounds composed of low-symmetric square cupola of Cu S=1/2 spins. We compared our theoretical results and the experimental data in collaboration with the experimental groups [1,2]. We have also studied a magnetoelectric effect in a heterostructure of band insulator and ferromagnet [3].

(ii) *Nonreciprocal transport*: We have unveiled nonreciprocal spin Seebeck responses in antiferromagnets on noncentrosymmetric lattices [4]. We have also elucidated a nonreciprocal spin transport in monoaxial chiral magnets, which would be useful as a spin-current diode in spintronics devices [5].

(iii) *Materials design by ab initio calculations*: Based on *ab initio* band calculations and model constructions, we have developed a generic theory for the e_g-orbital systems on a honeycomb structure. We found a plethora of peculiar band crossings, such as multiple Dirac nodes, semi-Dirac nodes, quadratic band crossings, and line nodes [6]. We have also proposed new candidate materials of *f*-electron systems for the Kitaev quantum spin liquids [7].

(iv) *Magnetic vortices and skyrmions*: We have clarified that both Neel- and Bloch-type magnetic vortices can appear in spin-orbit coupled metals, by using an effective spin model [8]. We extended the study to itinerant electron models and found interesting magnetic textures by a large-scale simulation [9]. We have also clarified the effect of magnetic anisotropy on the magnetic skyrmions with a high topological number of two [10].

(v) *Kitaev quantum spin liquids*: By using the Majorana mean-field theory, we have found successive phase transitions in the

antiferromagnetic Kitaev model while increasing an external magnetic field, where the Majorana fermionic states change their topology in the reciprocal space [11]. Also, upon our theoretical results obtained thus far, we have collaborated with several experimental groups for identifying the signatures of Majorana excitations in the Kitaev magnets: thermal Hall effect [12] and its half-quantization [13], Raman scattering [14], and nuclear quadrupole and magnetic resonances [15]. We have published a second article of our review on this topic [16].

References

[1] Y. Kato, K. Kimura, A. Miyake, M. Tokunaga, A. Matsuo, K. Kindo, M. Akaki, M. Hagiwara, S. Kimura, T. Kimura, and Y. Motome: Phys. Rev. B **99** (2019) 024415.

[2] K. Kimura, Y. Kato, K. Yamauchi, A. Miyake, M. Tokunaga, A. Matsuo, K. Kindo, M. Akaki, M. Hagiwara, S. Kimura, M. Toyoda, Y. Motome, and T. Kimura: Phys. Rev. Mat. **2** (2018) 104415, *Editors' Suggestion*.

[3] K. N. Okada, Y. Kato, and, Y. Motome, preprint (arXiv:1902.04204), accepted for the publication in Phys Rev. B.

[4] R. Takashima, Y. Shiomi, and Y. Motome: Phys. Rev. B **98** (2018) 020401(R).

[5] S. Okumura, H. Ishizuka, Y. Kato, J. Ohe, and Y. Motome, preprint (arXiv:1903.12358).

[6] Y. Sugita and Y. Motome, Phys. Rev. B **99** (2019) 041101(R).

[7] S.-H. Jang, R. Sano, Y. Kato, and Y. Motome, preprint (arXiv:1807.01443).

[8] S. Hayami and Y. Motome: Phys. Rev. Lett. **121** (2018) 137202, *selected as Cover image*.

[9] K. N. Okada, Y. Kato, and Y. Motome: Phys. Rev. B **98** (2018) 224406.

[10] S. Hayami and Y. Motome: Phys. Rev. B **99** (2019) 094420.

[11] J. Nasu, Y. Kato, Y. Kamiya, and Y. Motome: Phys. Rev. B **98** (2018) 060416(R).

[12] Y. Kasahara, K. Sugii, T. Ohnishi, M. Shimozawa, M. Yamashita, N. Kurita, H. Tanaka, J. Nasu, Y. Motome, T. Shibauchi, and Y. Matsuda, Phys. Rev. Lett. **120** (2018) 217205.

[13] Y. Kasahara, T. Ohnishi, Y. Mizukami, O. Tanaka, S. Ma, K. Sugii, N. Kurita, H. Tanaka, J. Nasu, Y. Motome, T. Shibauchi, and Y. Matsuda, Nature **559** (2018) 227.

[14] Y. Wang, G. B. Osterhoudt, Y. Tian, P. Lampen-Kelley, A. Banerjee, T. Goldstein, J. Yan, J. Knolle, J. Nasu, Y. Motome, S. Nagler, D. Mandrus, and K. S. Burch, preprint (arXiv:1809.07782).

[15] Y. Nagai, T. Jinno, Y. Yoshitake, J. Nasu, Y. Motome, M. Itoh, and Y. Shimizu, preprint (arXiv:1810.05379).

[16] 求 幸年, 那須 譲治: 固体物理 **53** (2018) 305.

Numerical studies on fractional excitations in strongly correlated electron systems

Youhei YAMAJI
Department of Applied Physics, the University of Tokyo
Hongo, Bunkyo-ku, Tokyo 113-8656

Fractionalized excitations have been actively studied in strongly correlated electron systems over the last several decades. The exploration of the fractionalized particles initiated by the discovery of the fractional quantum Hall effect has flourished and led to findings of exactly solvable many-body quantum systems such as the Kitaev model [1], which has been proposed to capture low-energy spin degrees of freedom in honeycomb networks of heavy transition metal ions typified by an iridium oxide Na_2IrO_3 and α-$RuCl_3$ [2].

Although these *relativistic* Mott insulators, Na_2IrO_3 and α-$RuCl_3$, exhibit spontaneous time-reversal symmetry breakings at low temperatures, their finite-temperature behaviors have been explained by assuming fractionalized Majorana excitations. The most characteristic signature of the fractionalization is the continuous spin excitation spectrum of α-$RuCl_3$ [3], in addition to the recent observation of the quantized thermal Hall effect [4].

Estimates of exchange couplings among ruthenium ions in α-$RuCl_3$ by using the density functional theory reveal that the dominant couplings are the Kitaev interaction and off-diagonal symmetric exchange coupling [5]. The off-diagonal symmetric coupling among $S = 1/2$ quantum spins on the honeycomb lattice is given by the following hamiltonian called the Γ model,

$$\hat{H} = \sum_{\gamma=x,y,z} \sum_{\langle i,j\rangle\in\gamma} \Gamma(\hat{S}_i^\alpha \hat{S}_j^\beta + \hat{S}_i^\beta \hat{S}_j^\alpha) \qquad (1)$$

where couplings for the nearest-neighbor bonds depend on the bond direction $\gamma = x, y, z$, (α, β, γ) is a permutation of (x, y, z), and Γ is the coupling constant and set as $\Gamma = 1$. To clarify the origin of the continuum in α-$RuCl_3$ and possible fractionalization, we examine spin dynamics dominated by the Γ model.

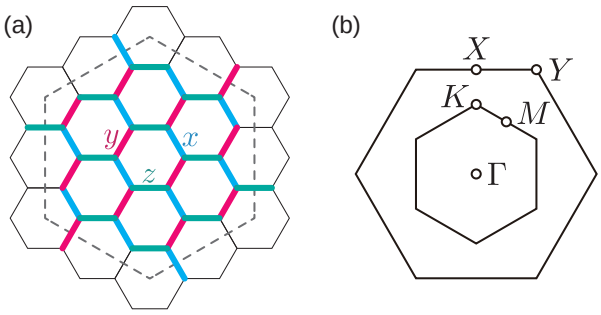

Figure 1: (a) 24 site cluster used in the present report. (b) Brillouin zone and high symmetry points of honeycomb lattices.

By applying the finite-temperature shifted Krylov subspace method [6], we simulate the exact dynamical spin structure factor $S(Q, \omega)$ of the Γ model for a 24 site cluster (see Fig. 1 (a)). At moderate temperatures $T = 0.5$, $S(Q, \omega)$ shows continuum, while suppression of low-energy spectral weight around the Γ and X points, as shown in Fig. 2 (a).

The continuum is interpreted as a combination of relaxational dynamics due to nearly degenerated exponentially degenerated low-energy states [7], which is also valid for the Kitaev model. As temperatures are lowered, the degeneracy is lifted and spin gaps seem to open as shown in Fig. 2 (b), (c), and (d), which

also resembles the spin gap opening in the Kitaev model.

The continuous spectra from the common origin in the Kitaev and Γ model indicates the existence of the fractionalized excitations even in the Γ model [7]. Further examination of the thermal Hall effect is desirable to elucidate the fractionalization.

References

[1] A. Kitaev: Ann. Phys. **321** (2006) 2.

[2] G. Jackeli and G. Khaliullin: Phys. Rev. Lett. **102** (2009) 017205.

[3] A. Banerjee, *et al.*: Science **356** (2017) 1055.

[4] Y. Kasahara, *et al.*: Nature **559** (2018) 227.

[5] For example, H.-S. Kim and H.-Y. Kee: Phys. Rev. B 93 (2016) 155143.

[6] Y. Yamaji, T. Suzuki, and M. Kawamura: arXiv:1802.02854.

[7] A. M. Samarakoon, G. Wachtel, Y. Yamaji, D. A. Tennant, C. D. Batista, and Y. B. Kim: Phys. Rev. B **98** (2018) 045121.

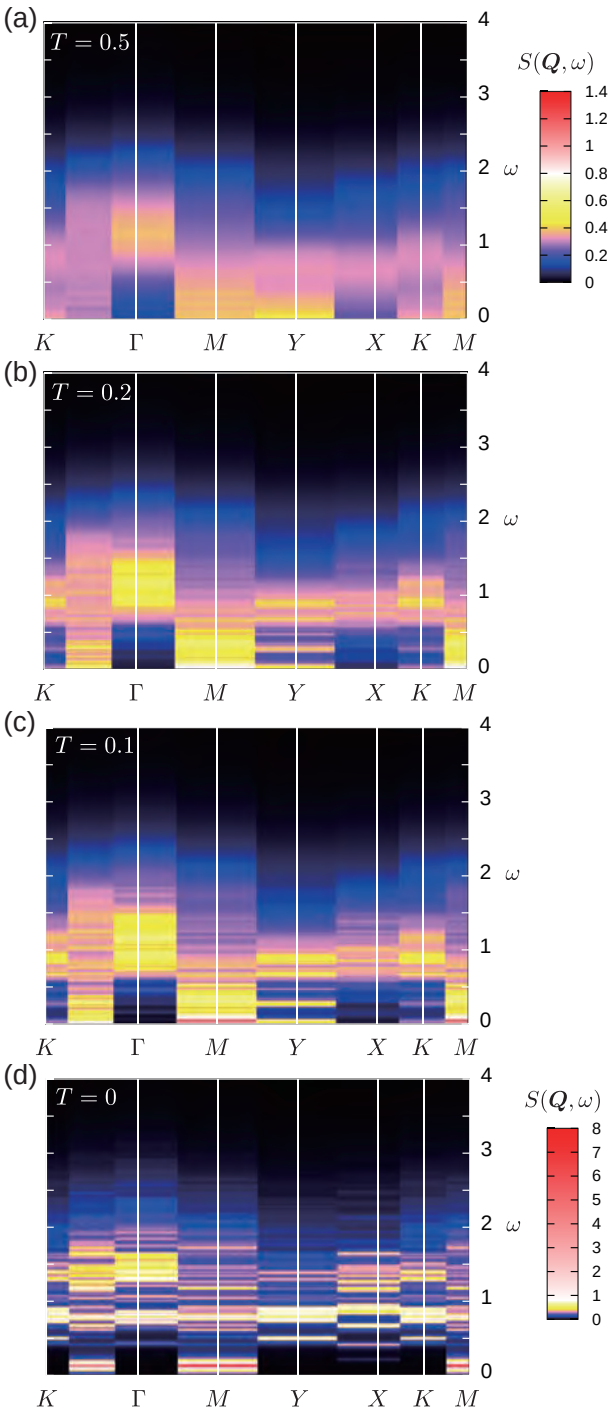

Figure 2: Finite-temperature $S(Q,\omega)$ along a path connecting high symmetry points defined in Fig. 1 (b), at $T = 0.5$ (a), $T = 0.2$ (b), $T = 0.1$ (c), and $S(Q,\omega)$ at $T = 0$ (d).

Study of magnetism and topological phase formation in strongly correlated quantum systems

Norio KAWAKAMI

Department of Physics,

Kyoto University, Kitashirakawa, Sakyo-ku, Kyoto 606-8502

We have studied strongly correlated quantum systems with focus on magnetism and topological phase formation.

(1) We have first explored topological states with magnetic order in heavy-fermion systems having a mirror symmetry. While in the absence of spatial symmetry topological phases cannot exist in two-dimensional (2D) antiferromagnetic phases, we have elucidated that in the presence of a mirror symmetry a topological phase emerges, and have explicitly shown this for a 2D periodic Anderson model. In the ferromagnetic phase around quarter filling, a half-metallic state with a spin-selective gap appears with properties characterized by a Chern number. [1]

(2) The observation of quantum oscillations in topological Kondo insulators SmB_6 and YbB_{12} is a recent puzzling experimental discovery. Quantum oscillations observed in the resistivity and the magnetization are usually explained by the existence of the Fermi surface. However, the Kondo insulators do not have a Fermi surface and thus should not show quantum oscillations. By performing real-space dynamical mean field calculations for topological Kondo insulators in a magnetic field, we have explored this problem. To include the effects of vector potential we need to enlarge the unit cell of the material to the magnetic unit cell consisting of 80-120 atoms.

We have clearly shown that the interplay between correlations and topology leads to observable quantum oscillations without the necessity of a Fermi surface. Particularly, we have shown that correlations strongly enhance the amplitude of quantum oscillations. The enhancement originates thereby in the renormalization of the band structure and finite lifetime of quasiparticles in the Landau levels away from the Fermi energy. We believe that this scenario can explain the observation of quantum oscillations in the magnetic torque for SmB_6 as well as oscillations in the resistivity and the magnetic torque of YbB_{12}. [2]

(3) Recent experiments indicate that, contrary to the long-standing belief, $CeCu_2Si_2$ is a heavy-fermion superconductor with a fully gapped s-wave superconducting state which may be caused by an on-site attractive pairing interaction. Motivated by this finding, we have investigated the competition between

superconductivity, charge-ordering, magnetic-ordering, and the Kondo effect in a heavy fermion s-wave superconductor described by a Kondo lattice model with an attractive on-site Hubbard interaction. At half filling, we have found an intriguing phase where the magnetic ordering of f-electrons lifts the degeneracy between the charge density wave (CDW) state and the superconducting state, leading to a strong suppression of superconductivity. In addition, the system may also become a half metal in this parameter regime. Away from half filling, the CDWs vanish and are replaced by superconductivity combined with incommensurate SDWs up to moderate Kondo couplings to the f-electrons. We have shown that both CDWs as well as superconductivity enhance magnetic ordering due to the suppression of Kondo screening. [3]

(4) It is known that the topological Kondo insulator SmB_6 becomes A-type anti-ferromagnetic under pressure. It is therefore not only an interesting theoretical question to analyze the phase diagram and the impact of magnetic states on the topological properties, but has also a direct impact on experiments. Using real-space dynamical mean field theory combined with numerical renormalization group for a three-dimensional topological Kondo insulator, we have found a wide ferromagnetic phase and an A-type anti-ferromagnetic phase. As has been studied in the topologically trivial Kondo lattice model, the ferromagnetic state exhibits a gap for one spin-direction, while the other spin direction becomes metallic. As in the previous study, we have found a gap for one spin direction in the topological Kondo insulator. Furthermore, because of the mirror symmetry, topological surface states are protected in the ferromagnetic state for the gapped spin direction. We have shown that the magnetic polarization deforms the surface Dirac cones, which can appear as surface Fermi arcs in the magnetic state. For the A-type antiferromagnetic state, we have found similar features in the spectrum, although the gap closes in this magnetic state, and thus the topological protection does not work. We believe that these results can be used to understand existing experiments and demonstrate new interesting experiments for SmB_6 under pressure. [4]

We note that Real-space DMFT maps the lattice on independent quantum impurity models, which must be solved self-consistently. Because all impurities can be solved parallel, the ISSP supercomputer can be efficiently used.

References

[1] K. Kimura, T. Yoshida, and N. Kawakami, J. Phys. Soc. Jpn. **87** (2018) 084705.

[2] R. Peters, T. Yoshida, and N. Kawakami, arXiv:1901.05099.

[3] B. Lechtenberg, R. Peters, and N. Kawakami, Phys. Rev. B **98** (2018) 195111.

[4] R. Peters, T. Yoshida, and N. Kawakami, Phys. Rev. B **98** (2018) 075104.

Numerical Studies on the Role of the Incipient Band Played in Multiband Superconductivity

KAZUHIKO KUROKI
Department of Physics, Osaka University
1-1 Machikaneyama, Toyonaka, Osaka, 560-0043, Japan

We have been theoretically persuing ideal situation for superconductivity in multiband systems. In ref.[1], we proposed that high-T_c superconductivity is possible in Hubbard-type systems (with the on-site U) having wide and narrow bands, where light effective mass and strong pairing interaction is realized when the Fermi level sits in the vicinity of, but does not intersect, the narrow band, namely, the incipient narrow band. The two-leg Hubbard ladder with diagonal hoppings, a model for the ladder-type cuprates, was studied as a system in which such a situation is realized, where a possible occurrence of high T_c superconductivity was suggested. More recently, we extended our study to various quasi-one-dimensional systems, and showed the that the incipient band mechanism of high T_c superconductivity works in a wide range of systems.[2].

In 2018 fiscal year, we have extended the study to two dimensional (2D) systems. A simplest extension of the two-leg ladder Hubbard model to two dimensions is the bilayer square lattice Hubbard model, where two Hubbard models on a square lattice are coupled by vertical hoppings t_r along with diagonal hoppings t'. Here, t' controls the band width of the narrow band, while t_r controls the relative energy between the two bands. We adopted the fluctuation exchange approximation, and invesigated a large parameter space of (t_r, t', n, U), where n is the band filling and U is the on-site Hubbard interaction. Simultaneously, we also performed similar calculation for the two-leg ladder Hubbard model, and made a comparison between the two models. In both cases, superconductivity is found to be strongly enhanced when the Fermi level sits close to the narrow band edge, namely, when the narrow band is incipient. The maximum T_c is expected to be about the same between the two. On the other hand, the parameter regime where T_c remains high is wider in the quasi 1D case. We have also studied bilayer models using triangular and honeycomb lattices, and found results similar to those for the square lattice. We have further extended our study to other multiband models, such as the checkerboard lattice, Lieb lattice, and Mielke lattice, and also to three dimensional lattices, where somewhat different results were obtained. We plan to publish the details of these results in the near future. Variational Monte Carlo study on the two-leg ladder and bilayer square lattices using the mVMC code is also underway.

The above mentioned study is based on purely theoretical models, and their relevance to actual materials is of great interest. In the past years, we have shown that a ladder-like electronic structure is hidden in the 3-2-7 Ruddlesden-Popper compounds, and proposed a possible occurrence of superconductivity in those materials.[3] In 2018 fiscal year, we started two other projects regarding actual materials. One is based on the cuprate ladder compounds, where we study the lattice deformation effects, and the other is based on a vanadium oxyhydride, where ladder-like electronic structure is realized. These studies are now underway.

As for the oxyhydrides, it is also important to understand how the hydrogen atoms affect the electron-electron interaction compared to that in the oxides. In 2018 fiscal year, we constructed low energy effective models for vanadium oxyhydrides $Sr_{n+1}V_nO_{2n+1}H_n$ ($n = 1$ and ∞),[4] where we evaluated the effective interaction using constrained RPA. The band structure was calculated using the Quantum ESPRESSO code, and the Wannier functions and the effective interactions were obtained using the RESPACK code. As low energy effective models, we consider the t_{2g} model, in which only the t_{2g} orbitals are explicitly considered, and the d model, where all the d orbitals are considered. We find that in the former model, the effective electron-electron interaction is strongly screened because the e_g bands are strongly entangled with the t_{2g} bands. On the other hand, in the latter model, the effective interaction is strong, due to the large separation between the d and the anion bands.

[1] K. Kuroki, T. Higashida, and R. Arita, Phys. Rev. B **72**, 212509 (2005).
[2] K. Matsumoto, D. Ogura, and K. Kuroki, Phys. Rev. B **97**, 014516 (2018).
[3] D. Ogura, H. Aoki, and K. Kuroki, Phys. Rev. B **96**, 184513 (2017).
[4] M. Ochi and K. Kuroki, Phys. Rev. B **99**, 155143 (2019).

Competition between superconductivity and orbital order emerging in strongly correlated electron

Akihisa Koga
Department of Physics, Tokyo Institute of Technology, Meguro, Tokyo 152-8551

Strongly correlated electron systems with multiorbitals have attracted much interest since they exhibit a variety of remarkable phenomena such as, *e.g.*, colossal magnetoresistance in manganites, or exotic superconductivity in ruthenates and iron pnictides. In these compounds, charge, spin, and orbital degrees of freedom are strongly coupled with each other, leading to the emergence of novel ordered states. A special class of multiorbital systems are the fullerene-based solids, which show an unconventional form of superconductivity in the vicinity of the Mott insulating state. In these compounds, triply degenerate electronic orbitals in fullerene molecules couple with vibration modes, resulting in a strong renormalization of the local interactions. The static interorbital interactions effectively become larger than the intraorbital interactions and a sign-inverted (antiferromagnetic) Hund coupling is realized. This negative Hund coupling is expected to play an essential role in stabilizing the unconventional superconductivity in these compounds, which stimulates further investigations on multiorbital systems.

Motivated by this, we have considered the three-orbital Hubbard model by applying dynamical-mean field theory. We have found in the phase diagram (see Fig. 1) the existence of spontaneously orbital-selective Mott and orbital-selective superconducting states [1], which may be relevant for understanding the low temperature properties of the fullerene-based solids. We have also considered translational symmetry breaking state in the three-orbital system [2]. An exotic criticality of the phase transition appears between the metallic and charge density wave (CDW) phases, where the CDW order parameter does not exhibit a conventional mean-field-like square root behavior. We have elucidated, using the Landau theory, that the CDW state is accompanied by the antiferro-orbital (AFO) order and the critical behavior is described by two order parameters, where the AFO order parameter is the primary order parameter and the CDW the secondary one.

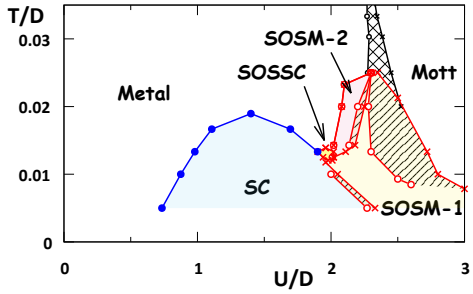

Figure 1: Phase diagram of the three orbital Hubbard model.

[C class 8000 (System B); 1450 (System C)]

References

[1] K. Ishigaki, J. Nasu, A. Koga, S. Hoshino, and P. Werner, Phys. Rev. B **98**, 235120 (2018).

[2] K. Ishigaki, J. Nasu, A. Koga, S. Hoshino, and P. Werner, Phys. Rev. B **99**, 085131 (2019).

Anomalous phenomena induced for correlated topological systems

Tsuneya Yoshida

Department of Physics,

1-1-1 Tennodai, Tsukuba, Ibaraki, JAPAN 305-8571

A variety of topological phenomena have been reported recently. In particular, for correlated systems, interplay between topology and correlations yields a rich physics. This report summarizes our recent studies with special emphasis on the following two points: (i) non-Hermitian phenomena in correlated systems; (ii) new topological states induced by interactions.

Let us start with our results obtained from non-Hermitian perspective on correlated systems. Our analysis based on the dynamical mean-field theory with the numerical renormalization group method have elucidated that correlated systems in equilibrium shows exceptional points in the single-particle spectrum [1]. We further have analyzed the non-Hermitian phenomenon by focusing on the interplay between exceptional points and symmetry. Our DMFT analysis has elucidated that the chiral symmetry of the honeycomb lattice induces a novel non-Hermitian degeneracies in the bulk which we call symmetry-protected exceptional rings[2]. Our

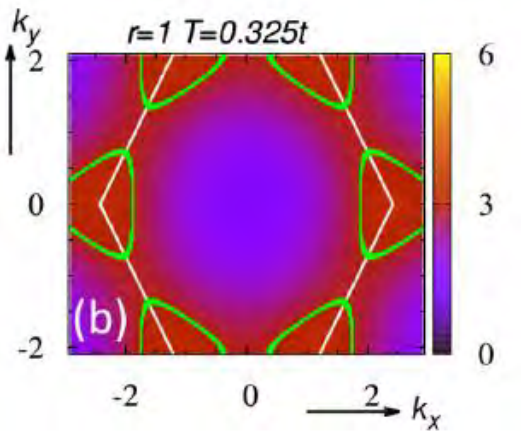

Fig.1 momentum resolved spectral weight in

scenario of the symmetry protection is quite degeneracies emerge for other symmetry classes and arbitrary dimensions.

Another aim of our studies is to reveal new topological phenomena induced by the interactions. Motivated by the recent experimental achievement, we have analyzed correlation effects on the topological pump for one-dimensional Rice-Mele model. Our DMRG analysis elucidates the jump of the polarization splits with maintaining the Chern number. This results indicates that the split of the jump is the signal of topological Mott behaviors for the

topological pump[3]. We also have discovered new topological states induced by reflection symmetry and Coulomb interactions, topological mirror Kondo metals [4,5]. In addition, we have proposed an experimental setup for cold atoms allowing us to observe the reduction of topological classification Z to Z_4[6].

References

[1] T. Yoshida, R. Peters, and N. Kawakami, Phys. Rev. B **98** (2018) 035141.

[2] T. Yoshida, R. Peters, N. Kawakami, and Y. Hatsugai, Phys. Rev. B **99** (2019) 121101.

[3] M. Nakagawa T. Yoshida, R. Peters, and N. Kawakami, Phys. Rev. B **98** (2018) 115147.

[4] R. Peters, T. Yoshida, and N. Kawakami, Phys. Rev. B **98** (2018) 075104.

[5] K. Kimura, T. Yoshida, and N. Kawakami, J. Phys. Soc. Jpn. **87**, (2018) 084705.

[6] T. Yoshida, I. Danshita, R. Peters, and N. Kawakami, Phys. Rev. Lett. **121** (2018) 025301.

Effect of magnetic anisotropy on skyrmion crystal in the Kondo lattice model

Satoru Hayami
Department of Physics, Hokkaido University, Sapporo, 060-0810

Noncollinear and noncoplanar magnetic orderings have drawn considerable interest in condensed matter physics. A noncollinear magnetic order shows the vector chirality defined by a vector product of spins and a noncoplanar magnetic order shows the scalar chirality defined by a triple scalar product of spins. Among them, the spin scalar chirality has recently attracted much interest, since it leads to an emergent electromagnetic field for electrons through the spin Berry phase mechanism [1, 2, 3]. Skyrmion crystals are one of the fundamental examples to possess such a scalar chirality degree of freedom [4].

Recently, several theoretical studies show that such a skyrmion crystal is stabilized even in the Kondo lattice model in centrosymmetric systems [5, 6, 7]. For instance, it is found that a skyrmion crystal with a high topological number of two is realized at zero magnetic field in the Kondo lattice model on a triangular lattice [8, 9]. Moreover, this skyrmion crystal phase shows phase transitions with successive changes of the topological number $2 \to 1 \to 0$ with an increase of a magnetic field. Meanwhile, such a skyrmion crystal with the topological number of two has yet to be found in experiments. Thus, it is useful to examine how the skyrmion crystal with the topological number of two in itinerant magnets is robust against perturbations, such as magnetic anisotropy, in order to search for an optimal condition for its stabilization.

In this project, we investigate the effect of a single-ion anisotropy on the skyrmion crystal phase in itinerant magnets. We examine how the spin structures in the skyrmion crystal phase are modulated and how these topological phases are robust against introducing easy-axis and easy-plane anisotropy [10]. To this end, we consider the Kondo lattice model including the single-ion anisotropy and external magnetic field on the triangular lattice. The Kondo lattice Hamiltonian is given by

$$\begin{aligned}\mathcal{H} = & - \sum_{i,j,\sigma} t_{ij} c^{\dagger}_{i\sigma} c_{j\sigma} + J \sum_{i} \mathbf{s}_i \cdot \mathbf{S}_i \\ & - A \sum_{i} (S^z_i)^2 - \sum_{i} \mathbf{H} \cdot \mathbf{S}_i, \end{aligned} \tag{1}$$

where $c^{\dagger}_{i\sigma}$ ($c_{i\sigma}$) is a creation (annihilation) operator of an itinerant electron at site i and spin σ. The first term represents the kinetic energy of itinerant electrons. We consider hopping elements between nearest-neighbor sites, $t_{ij} = t_1 = 1$, and third-neighbor sites, $t_{ij} = t_3 = -0.85$. The second term represents the onsite exchange coupling between itinerant electron spins $\mathbf{s}_i = (1/2) \sum_{\sigma,\sigma'} c^{\dagger}_{i\sigma} \boldsymbol{\sigma}_{\sigma\sigma'} c_{i\sigma'}$ and localized spins $\mathbf{S}_i$ with a coupling constant J, where $\boldsymbol{\sigma} = (\sigma^x, \sigma^y, \sigma^z)$ is the vector of Pauli matrices. We consider $\mathbf{S}_i$ as a classical spin with fixed length $|\mathbf{S}_i| = 1$. The third and fourth terms represent the easy-axis ($A > 0$) or easy-plane ($A < 0$) anisotropy and the Zeeman coupling to an external magnetic field along the z direction, which are taken into account only for the localized spins for simplicity. We set the chemical potential $\mu = -3.5$.

We investigate the ground-state phase diagram of the Kondo lattice model in Eq. (1) on the triangular lattice by performing large-

scale Langevin dynamics simulations enabled by the kernel polynomial method (KPM-LD), which enables us to calculate for large system sizes [11, 12]. Our simulation is done at zero temperature from random spin configurations for a 96^2-site cluster of the triangular lattice with periodic boundary conditions in both directions. In the KPM-LD simulations, we expand the density of states by up to 2000th order of the Chebyshev polynomials with 16^2 random vectors and we use a projected Heun scheme for 1000-5000 steps with the time interval $\Delta\tau = 2$.

As a result, we find that the spin textures on the skyrmion crystal phase with the topological number of two at zero field are deformed so as to consist of the magnetic vortices in the xy spin component and the sinusoidal wave in the z spin component [10]. In addition, we show that the skyrmion crystal phase shows a topological phase transition into the single-Q collinear in the z spin component (double-Q noncoplanar) state under easy-axis (easy-plane) anisotropy. We also show that the skyrmion crystals with the topological number of two and one show different behaviors in an applied magnetic field in the presence of single-ion anisotropy. The stable magnetic field range of the skyrmion crystal with the topological number of two is rather insensitive to the single-ion anisotropy, while the stable magnetic field region of the skyrmion crystal with the topological number of one is considerably extended (reduced) by the easy-axis (easy-plane) anisotropy, which is similar to the skyrmion crystals found in frustrated magnets. Our result indicates that the unconventional skyrmion crystal with the topological number of two in itinerant magnets is expected to be found in materials with a relatively small spin-charge coupling compared to the bandwidth and small magnetic anisotropy.

References

[1] D. Loss and P. M. Goldbart, Phys. Rev. B **45**, 13544 (1992).

[2] J. Ye, Y. B. Kim, A. J. Millis, B. I. Shraiman, P. Majumdar, and Z. Tešanović, Phys. Rev. Lett. **83**, 3737 (1999).

[3] K. Ohgushi, S. Murakami, and N. Nagaosa, Phys. Rev. B **62**, R6065(R) (2000).

[4] N. Nagaosa and Y. Tokura, Nat. Nanotechnol. **8**, 899 (2013).

[5] I. Martin and C. D. Batista, Phys. Rev. Lett. **101**, 156402 (2008).

[6] Y. Akagi and Y. Motome, J. Phys. Soc. Jpn. **79**, 083711 (2010).

[7] R. Shindou and N. Nagaosa, Phys. Rev. Lett. **87**, 116801 (2001).

[8] R. Ozawa, S. Hayami, and Y. Motome, Phys. Rev. Lett. **118**, 147205 (2017).

[9] S. Hayami, R. Ozawa, and Y. Motome, Phys. Rev. B **95**, 224424 (2017).

[10] S. Hayami and Y. Motome, Phys. Rev. B **99**, 094420 (2019).

[11] K. Barros and Y. Kato, Phys. Rev. B **88**, 235101 (2013).

[12] A. Weiße, G. Wellein, A. Alvermann, and H. Fehske, Rev. Mod. Phys. **78**, 275 (2006).

Development of powerful numerical methods for strongly-correlated systems

Yusuke NOMURA

Department of Applied Physics,

The University of Tokyo, Hongo, 7-3-1, Bunkyo-ku, Tokyo 113-8656

Developing powerful numerical methods for solving strongly-correlated Hamiltonians is a great challenge in condensed matter physics. In this fiscal year, we focus on the development of i) multi-orbital TRILEX (triply irreducible local expansion) and ii) machine learning solvers for electron-phonon coupled systems.

i) Development of multi-orbital TRILEX

TRILEX is a method which can interpolate weak-coupling and strong-coupling approaches of Green's function method [1]. In the TRILEX, we calculate the local irreducible vertex, which is usually neglected in the weak-coupling approach. In the weakly-correlated region, the vertex is almost frequency independent and the TRILEX methods reproduces spin-fluctuation and GW methods. At the same time, the TRILEX can capture Mott physics: strong frequency dependence of the local vertex induces Mott transition.

So far, the TRILEX has been applied to single-band model. In the present study, we extend the TRILEX to multi-orbital models. In multi-orbital systems, we calculate the vertex for not only charge/spin channel but also orbital channel. Then, we can investigate the competition/interplay among charge, spin, and orbital degrees of freedom. We perform benchmark calculations using $SrVO_3$, a typical strongly correlated metal. In future, we are planning to perform calculations for iron-based superconductors.

ii) Machine learning solvers for electron-phonon coupled systems

Recently, variational wave function written in terms of restricted Boltzmann machine (RBM) has been introduced to represent ground states of quantum spin Hamiltonians [2]. The RBM wave function has been shown to be able to represent ground states of spin Hamiltonians in high accuracy [2]. We extend this machine learning scheme to the electron-phonon coupled systems.

In the wave functions used so far for electron-coupled systems, the correlation between electrons and phonons are taken into account only by correlation factors [3,4]. In the present study, we first prepare entangled vibronic wave functions and more sophisticated correlations between electrons and phonons are taken into account by the RBM. Compared to the wave function proposed in Ref. [3], the improved

wave function substantially improve the accuracy of the ground state energy of one-dimensional Holstein model.

References

[1] T. Ayral and O. Parcollet, Phys. Rev. B **92**, 115109 (2015).

[2] G. Carleo and M. Troyer, Science **355**, 602 (2017).

[3] T. Ohgoe and M. Imada, Phys. Rev. B **89**, 195139 (2014).

[4] S. Karakuzu et al., Phys. Rev. B **96**, 205145 (2017)

Multi-channel Kondo effect in rare-earth systems

Takashi HOTTA
Department of Physics, Tokyo Metropolitan University
1-1 Minami-Osawa, Hachioji, Tokyo 192-0397

In this research, we have analyzed a seven-orbital impurity Anderson model hybridized with Γ_8 conduction electrons by employing a numerical renormalization group (NRG) technique. The model Hamiltonian is given by

$$\begin{aligned} H &= \sum_{\mathbf{k},\mu,\tau} \varepsilon_{\mathbf{k}} c^\dagger_{\mathbf{k}\mu\tau} c_{\mathbf{k}\mu\tau} + \sum_{\mathbf{k},\mu,\tau} V(c^\dagger_{\mathbf{k}\mu\tau} f_{a\mu\tau} + \text{h.c.}) \\ &+ \sum_{j,\mu,\tau} (\lambda_j + B_{j,\mu} + E_f) f^\dagger_{j\mu\tau} f_{j\mu\tau} \\ &+ \sum_{j_1\sim j_4} \sum_{\mu_1\sim\mu_4} \sum_{\tau_1\sim\tau_4} I^{j_1 j_2, j_3 j_4}_{\mu_1\tau_1\mu_2\tau_2,\mu_3\tau_3\mu_4\tau_4} \\ &\times f^\dagger_{j_1\mu_1\tau_1} f^\dagger_{j_2\mu_2\tau_2} f_{j_3\mu_3\tau_3} f_{j_4\mu_4\tau_4}, \end{aligned} \tag{1}$$

where $\varepsilon_{\mathbf{k}}$ is the dispersion of a Γ_8 conduction electron with wave vector $\mathbf{k}$, $c_{\mathbf{k}\mu\tau}$ denotes the annihilation operator of a Γ_8 conduction electron, μ distinguishes the cubic irreducible representation, Γ_8 states are distinguished by $\mu = \alpha$ and β, while Γ_7 and Γ_6 states are labeled by $\mu = \gamma$ and δ, respectively, τ is the pseudo-spin which distinguishes the degeneracy concerning the time-reversal symmetry, $f_{j\mu\tau}$ indicates the annihilation operator of a localized f electron in the bases of (j, μ, τ), j is the total angular momentum, $j = 5/2$ and $7/2$ are denoted by "a" and "b", respectively, and V is the hybridization between conduction and localized electrons. In the present case, we consider the hybridization between Γ_8 conduction electrons and the Γ_8 quartet of $j = 5/2$.

Concerning the local f-electron terms of Eq. (1), $\lambda_a = -2\lambda$, $\lambda_b = (3/2)\lambda$, λ is the spin-orbit coupling of f electron, $B_{j,\mu}$ denotes the crystalline electric field (CEF) potential energy, E_f indicate the f-electron level, and I denotes the Coulomb interactions between f electrons. The Coulomb interaction I is expressed with the use of four Slater-Condon parameters, F^0, F^2, F^4, and F^6. Although the Slater-Condon parameters of a material should be determined from experimental results, here we simply set the ratio as $F^0/10 = F^2/5 = F^4/3 = F^6 = U$, where U is the Hund rule interaction among f orbitals. The CEF potentials for f electrons from ligand ions are given in the table of Hutchings for the angular momentum $\ell = 3$. For a cubic structure with $O_{\rm h}$ symmetry, CEF parameters are expressed by two CEF parameters, B^0_4 and B^0_6.

As U denotes the magnitude of the Hund rule interaction among f orbitals, it is reasonable to set $U = 1$ eV. The magnitude of λ varies between 0.077 and 0.36 eV depending on the type of lanthanide ions. In the following, B^0_4 and B^0_6 are treated as parameters. To control the local f-electron number n, we appropriately adjust the value of E_f.

In this study, we analyze the model by employing the NRG method. We introduce a cut-off Λ for the logarithmic discretization of the conduction band. Owing to the limitation of computer resources, we keep M low-energy states. Here, we use $\Lambda = 5$ and $M = 4,000$. In the following calculations, the energy unit is D, which is a half of the conduction band width. Namely, we set $D = U = 1$ eV in this calculation. In the NRG calculation, the temperature T is defined as $T = \Lambda^{-(N-1)/2}$ in the present energy unit, where N is the number of renormalization steps.

In our previous research, we have investigated the two-channel Kondo effect for the

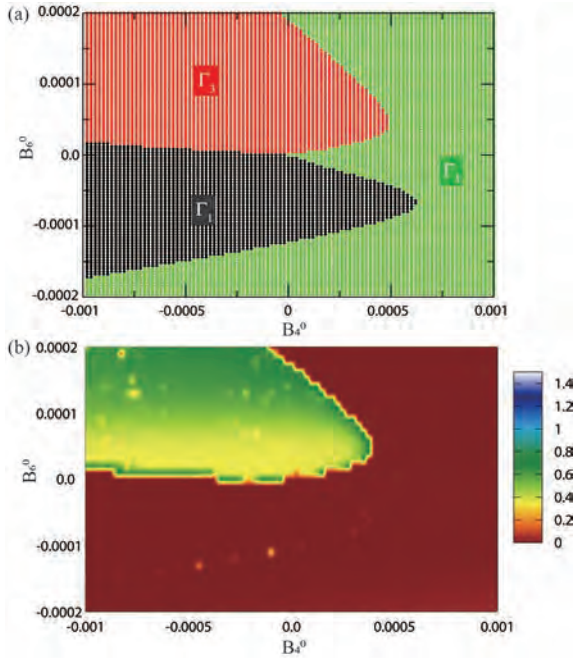

Figure 1: (a) Local CEF ground-state phase diagram for $n = 4$. (b) Contour color map of the entropy on (B_4^0, B_6^0) plane for $V = 0.87$ and $T = 5.12 \times 10^{-7}$.

case of $n = 2$, corresponding to Pr^{3+} ion [1]. We have reconfirmed the emergence of the quadrupole two-channel Kondo effect, as first remarked by Cox, when there appears the local Γ_3 ground state. We have also considered the case of $n = 3$, corresponding to Nd^{3+} ion [2]. For the case of $n = 3$ with the local Γ_6 ground state, we have discovered the magnetic two-channel Kondo effect.

Next we consider the case of $n = 4$, corresponding to Pm^{3+} ion. Although promethium has no stable isotopes, it is rather adequate to consider Np^{3+} or Pu^{3+} ion with $5f^4$ configuration. Here we show the results for $n = 4$. In Fig. 1(a), we depict local CEF ground-state phase diagram on the plane of B_4^0 and B_6^0. The region with Γ_3 ground state is widely observed for $B_6^0 > 0$.

In Fig. 1(b), we show the contour color map of the entropy for $V = 0.87$ and $T = 5.12 \times 10^{-7}$. To visualize precisely the behavior of entropy, we define the color of the entropy between 0 and 1.5, as shown in the right color bar. We immediately notice that a region with an entropy of $0.5 \log 2$ (yellow region) almost corresponds to that of the Γ_3 ground state in comparison with Fig. 1(a). Note that for large B_6^0, the color becomes green, but when we decrease the temperature, we find the entropy of $0.5 \log 2$ even for large B_6^0. The results strongly suggest the emergence of quadrupole two-channel Kondo effect for the case of $n = 4$.

Note that in the region of $B_6^0 < 0$, we observe some blurry yellow spots along the boundary region between Γ_1 singlet and Γ_5 triplet local ground states. These denote the quantum critical points, which are generally known to appear between the local CEF and Kondo singlet states.

As for the mechanism of quadrupole two-channel Kondo effect for the case of $n = 4$, we deduce that it is essentially the same as that for the case of $n = 2$ on the basis of a j-j coupling scheme. When we accommodate four electrons in the $j = 5/2$ sextet, we immediately notice that it just denotes the configuration of two holes in the sextet. Namely, the electron-hole relation on the basis of the j-j coupling scheme should be a key issue to understand the two-channel Kondo effect emerging from rare-earth ions. For the case of heavy rare-earth ions corresponding to $n = 8 \sim 12$, we believe that the present idea will be also effective. This point will be discussed in future elsewhere [3].

References

[1] T. Hotta, Physica B **536C**, 203-210 (2018).

[2] T. Hotta, J. Phys. Soc. Jpn. **86**, 083704 (2017).

[3] D. Matsui and T. Hotta, in preparation.

First-principles calculation and dynamical mean-field theory for superconductivity in multi-band systems

Yoshiaki Ōno
Department of Physics, Niigata University
Ikarashi, Nishi-ku, Niigata, 950-2181

Recently, the ternary chalcogenide Ta_2NiSe_5 has received renewed attention as a strong candidate for the excitonic insulator (EI) which is characterized by the condensation of excitons and has been argued for about half a century. The resistivity indicates a narrow gap semiconductor with a quasi one-dimensional (1-D) structure where a Ni chain and adjacent two Ta chains construct the 1-D three chain. A second-order structural transition from the orthorhombic to monoclinic phase occurs at a critical temperature T_S=328 K, below which a remarkable flattening of the valence band top is observed in the ARPES experiment without any sign of the magnetic and density-wave-type order. Several theoretical studies have revealed that the transition is well accounted for by the excitonic condensation from a normal semiconductor (orthorhombic) to the EI (monoclinic) from a mean-field analysis for the 1-D three-chain Hubbard model and from a variational cluster approximation for the extended Falicov-Kimball model. Recent optical measurements are also consistent with the EI phase below T_S.

When the pressure is applied for Ta_2NiSe_5, T_S is suppressed and the system changes from semiconducting to semimetallic both above and below T_S, and then, T_S finally becomes zero at a critical pressure $P_c \sim 8$GPa, around which the superconductivity is observed. Then, we have recently investigated the 1-D three-chain Hubbard model also in the semimetallic case and have found that the difference of the band degeneracy, the two-fold degenerate conduction bands and the nondegenerate valence band, inevitably causes the imbalance of each Fermi wavenumber and results in a remarkable excitonic state characterized by the condensation of excitons with finite center-of-mass momentum q, the so-called Fulde-Ferrell-Larkin-Ovchinnikov (FFLO) excitonic state[1, 2], as previously discussed in the electron-hole bilayer systems with density imbalance. More recently, a realistic quasi 1-D three-chain Hubbard model has also been studied and a detailed excitonic phase diagram including the FFLO state has been obtained[3].

As the superconductivity is observed near the excitonic phase in Ta_2NiSe_5, the excitonic fluctuation is considered to be a key ingredient for the pairing mechanism as early discussed by Little for quasi 1-D organic superconductors but has not been discussed for Ta_2NiSe_5 so far. Then, we investigte the excitonic fluctuation and its mediated superconductivity in Ta_2NiSe_5 on the basis of the quasi 1-D three-chain Hubbard model[4] where the FFLO excitonic order is found to take place in the semimetallic case[3]. In the semimetallic case where two conduction (c) bands and one valence (f) band cross the Fermi level, the c-f Coulomb interaction drives the instability towards the Fulde-Ferrell-Larkin-Ovchinnikov (FFLO) excitonic order characterized by the condensation of excitons with finite center-of-mass momentum corresponding to the nesting between the c and

f Fermi surfaces. Near the instability, the largely enhanced excitonic fluctuations mediate the c-f interband Cooper pairs with finite center-of-mass momentum resulting in the FFLO superconductivity[4], which is expected to be realized in the semimetallic Ta_2NiSe_5 under high pressure.

References

[1] T. Yamada, K. Domon, and Y. Ōno, J. Phys. Soc. Jpn. **85**, 053703 (2016).

[2] K. Domon, T. Yamada, and Y. Ōno, J. Phys. Soc. Jpn. **85**, 065005 (2016).

[3] K. Domon, T. Yamada, and Y. Ōno, J. Phys. Soc. Jpn. **87**, 054701 (2018).

[4] T. Yamada, K. Domon, and Y. Ōno, J. Phys. Soc. Jpn. in press.

Superconductivity and magnetic properties of the Hubbard model

Atsushi Yamada
Department of Physics, Chiba University
Chiba 263-8522, Japana, Chiba 277-8581

The interplay of electron correlations, low dimensionality, and frustrated magnetic interactions lead to a rich variety of phenomena. For example, a spin liquid state, which is a purely non-magnetic Mott insulator without spontaneously broken spatial or spin symmetry, has attracted a lot of interest. This state is realized in geometrically frustrated systems like the charge organic transfer salts κ-(BEDT-TTF)$_2$X[1] and Cs_2CuCl_4.[2] A simple theoretical model of these compounds is the Hubbard model on the an-isotropic triangular lattice, and spin liquid state is in fact found in this model.[3] A spin liquid could arise also in the intermediate coupling region of strongly correlated systems between a semimetal and ordered state, because in this case a correlation-driven insulating gap might open before the system becomes ordered. This possibility might be realized in the half-filled Hubbard model on the honeycomb lattice.

We have studied the magnetic and metal-to-insulator transitions in the half-filled Hubbard model on the honeycomb lattice by variational cluster approximation using 10-site and 16-site clusters as a reference system.[5] Our method uses an exact diagonalization of the Hubbard model defined on these clusters and parts of numerical calculations were done using the computer facilities of the ISSP.Our results agree with recent large scale Quantum Monte Carlo simulations.[4] We are currently improving our program to study superconductivity.

References

[1] Y. Shimizu, K. Miyagawa, K. Kanoda, M. Maesato, and G. Saito, Phys. Rev. Lett. **91**, 107001 (2003); Y. Kurosaki, Y. Shimizu, K. Miyagawa, K. Kanoda, and G. Saito, Phys. Rev. Lett. **95**, 177001 (2005).

[2] R. Coldea, D.A. Tennant, A.M. Tsvelik, and Z. Tylczynski, Phys. Rev. Lett. **86**, 1335 (2001); R. Coldea, D.A. Tennant, and Z. Tylczynski, Phys. Rev. Lett. **68**, 134424 (2003).

[3] T. Yoshioka, A. Koga, and N. Kawakami, Phys. Rev. Lett. **103**, 036401 (2009); P. Sahebsara and D. Sénéchal, Phys. Rev. Lett. **100**, 136402 (2008); L.F. Tocchio, H. Feldner, F. Becca, R. Valenti, and C. Gros, Phys. Rev. B **87**, 035143 (2013); A. Yamada, Phys. Rev. B **89**, 195108 (2014); L.F. Tocchio, C. Gros, R. Valentí, F. Becca, Phys. Rev. B **89**, 235107 (2014); A. Yamada, Phys. Rev. B **90**, 235138 (2014).

[4] S. Sorella, Y. Otsuka, and S. Yunoki, Sci. Rep. **2**, 992 (2012); F. F. Assaad and I. F. Herbut, Phys. Rev. X **3**, 031010 (2013); F. Parisen Toldin, M. Hohenadler, F. F. Assaad, and I. F. Herbut, Phys. Rev. B **91**, 165108 (2015).

[5] A. Yamada, Int. J. Mod. Phys. B **30**, 1650158 (2016).

Numerical approach to unconventional electronic orderings in strongly correlated systems

Shintaro HOSHINO
Department of Physics, Saitama University, Saitama 338-8570, Japan

In A_3C_{60}, three electrons are doped onto each fullerene molecule from intercalated alkaline metals denoted by A [1, 2]. In the metallic compounds, the molecular t_{1u} orbitals form three half-filled narrow bands, and the electronic correlations are strong. Even though the symmetry of the pairing state is s-wave, the superconductivity is different from that of conventional BCS superconductors. Furthermore, fullerides exhibit a superconducting dome in the vicinity of a Mott insulating phase, which is a characteristic feature for the strongly-correlated superconductors. An important ingredient in the superconducting mechanism is an effectively sign-reversed Hund's coupling. This antiferromagnetic Hund's coupling favors the low-spin ($S = 1/2$) state, which has doubly occupied orbitals and can act as a seed for superconductivity.

Recent experiments have revealed the existence of a highly anomalous metallic state near the Mott transition [3]. When the electrons are localized in the Mott phase, the electron-phonon coupling leads to a deformation of the fullerene molecule. On the other hand, in the conventional metallic regime, the molecules exhibit a nearly spherical shape. In the regime between the Mott phase and weak-coupling metal, a deformation of the fullerene molecules has been detected with the metallic property [called Jahn-Teller metal (JTM)].

We have studied the three-orbital Hubbard model with antiferromagnetic Hund's coupling [4], by using the dynamical mean-field theory combined with continuous-time quantum Monte Carlo (DMFT+CTQMC) [5]. This study proposed that the JTM may be interpreted as a spontaneous orbital-selective Mott (SOSM) state, in which the localized and itinerant electrons coexist, explaining the basic properties of the JTM. The large-scale parallelized calculation using the supercomputer in ISSP is very efficient for DMFT+CTQMC since the method is based on the Monte Carlo sampling. Recently, the technique is effectively used to further clarifying the various ordered phases in the three-orbital Hubbard model [6, 7]. We are also performing the calculation using the realistic band structure in Ref. [8], to investigate the quantitative properties in fullerides. This theoretical study will enable us to compare the obtained molecular-orbital properties with experiments directly.

References

[1] M. Capone *et al.*, Rev. Mod. Phys. 81, 943 (2009).

[2] Y. Nomura *et al.*, J. Phys.: Condens. Matter 28, 153001 (2016).

[3] R.H. Zadik *et al.*, Sci. Adv. **1**, e1500059 (2015).

[4] S. Hoshino and P. Werner, Phys. Rev. Lett. **118**, 177002 (2017).

[5] E. Gull *et al.*, Rev. Mod. Phys. **83**, 349 (2011).

[6] K. Ishigaki *et al.*, Phys. Rev. B **98**, 235120 (2018).

[7] K. Ishigaki *et al.*, Phys. Rev. B **99**, 085131 (2019).

[8] Y. Nomura, K. Nakamura and R. Arita, Phys. Rev. B **85**, 155452 (2012).

First-principles calculations of $5d$ pyrochlore oxides

Hiroshi Shinaoka
Department of Physics, Saitama University, Saitama 338-8570

We focused on the pyrochlore oxides $Cd_2Re_2O_7$ using massive parallel computer simulations. $Cd_2Re_2O_7$ has been attracting much attention because the compound hosts a variety of phases at ambient pressure and high pressures including multipole ordered states [1, 2].

First, we constructed a tight-binding model for the t_{2g} manifold in terms of maximally localized Wannier functions (MLWF). The calculations were done for the lattice constant of $a = 10.226$ Å and the internal parameter of $x(O_1) = 0.318$. We used the open-source DFT package Quantum ESPRESSO and Wannier90. Figure 1 compares the LDA (local density approximation) band structure and the fit by Wannier functions, where one can see a good agreement for the t_{2g} band near the Fermi level. The computed LDA band structure is consistent with that obtained in a previous study [3].

We analyzed the structure of the tight-binding Hamiltonian in real space. Figure 2 shows how their absolute values decay with respect to distance. A conventional face-centered cubic unit cell of the crystal structure is also shown. Although they decay roughly exponentially, we found two pronounced peaks around $r/a = \sqrt{2}/4$ and $3\sqrt{2}/4$. A closer look indicates that they correspond to hopping along one-dimensional chains shown in Fig. 2. A similar structure was found for a related compound $Cd_2Os_2O_7$.

We estimated the strength of the trigonal crystal field Δ and the spin-orbit coupling ζ in the t_{2g} manifold. We used the same notation as employed in a previous study [4]. The results are summarized in Table I. As reference data, we estimated the parameters for $Cd_2Os_2O_7$ and obtained values consistent with the previous study [5]. The values of Δ and ζ for $Cd_2Re_2O_7$ are close to those for $Cd_2Os_2O_7$. The trigonal crystal field and the spin-orbit coupling are comparable in strength.

We are planning to analyze the strongly correlated aspects of the compound using the open-source software `DCore` [6], which was developed in Project for advancement of software usability in materials science [7] in the fiscal year of 2017.

This study was done in collaboration with N. Chikano, Y. Nomura, J. Otsuki, K. Yoshimi.

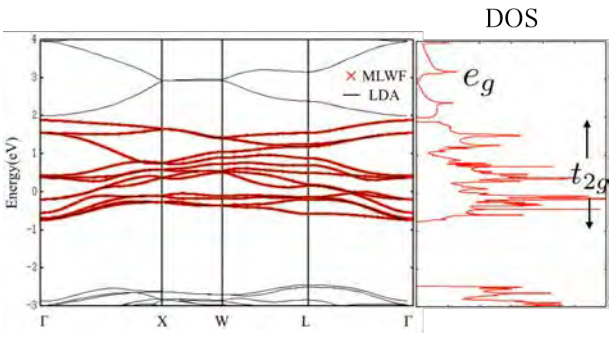

Figure 1: LDA band structure of $Cd_2Re_2O_7$.

References

[1] J. W. Harter, Z. Y. Zhao, J.-Q. Yan *et al.*, Science **356**, 295 (2017).

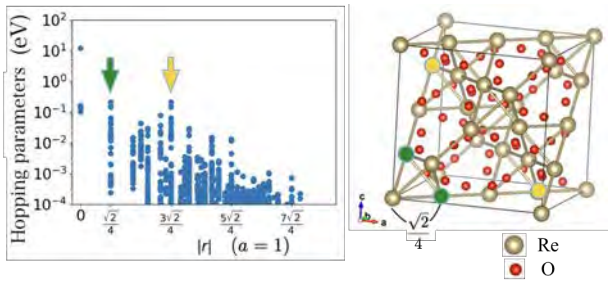

Figure 2: Analysis of elements of the hopping matrix.

	($5d^2$)	($5d^3$)	
	$Cd_2Re_2O_7$	$Cd_2Os_2O_7$	$Cd_2Os_2O_7$※
λ[eV]	0.31	0.34	0.33
Δ[eV]	0.23	0.18	0.19
$x(O(1))$	0.318	0.319	

※ A. Uehara, H. Shinaoka, Y. Motome, Physics Procedia **75**, 495-502 (2015).

Table 1: Estimated values of the spin-orbit coupling λ and the trigonal crystal field Δ.

[2] Z Hiroi, J Yamaura, T C. Kobayashi *et al.*, JPSJ **87**, 024702 (2018) and references therein.

[3] H. Harima, J. Phys. Chem. Solids **63**, 1035 (2002).

[4] H. Shinaoka, Y. Motome, T. Miyake, and S. Ishibashi, PRB **88**, 174422 (2013).

[5] A. Uehara, H. Shinaoka, Y. Motome, Physics Procedia **75**, 495 (2015).

[6] `https://github.com/issp-center-dev/DCore`

[7] `http://www.issp.u-tokyo.ac.jp/supercom/softwaredev`

Spin glass transition at finite temperature in the two dimensional transverse Ising model

Chisa Hotta
Department of Basic Science, University of Tokyo
Meguro-ku, Komaba, Tokyo 153-8902

We studied the quantum transverse Ising model on a triangular lattice with quenched bond randomness using the ISSP supercomputer system. Our Hamiltonian is given as

$$H = \sum_{\langle i,j \rangle} J_{ij}\sigma_i^z\sigma_j^z + \sum_{i=1}^{N} \Gamma\sigma_i^x, \qquad (1)$$

where σ_i^α ($\alpha = x, y, z$) is the Pauli operator on site-i, J_{ij} is the random Ising interaction with $\bar{J_{ij}} = 1$, and Γ is the transverse field. The degree of randomness R is defined as the half width of the distribution of J_{ij}.

The difficulty of obtaining reliable results in the disordered system is already well known in the long history of the classical spin glass[1]. In classical Edwards Anderson models, the spin glass transition is studied by the spin glass susceptibility and the replica overlap,

$$\chi_{\rm SG} = \frac{1}{N}\sum_{i,j=1}^{N} \langle\sigma_i^z\sigma_j^z\rangle^2, \qquad (2)$$

$$q_{\alpha\beta} = \sum_i \sigma_{i;\alpha}^z\sigma_{i;\beta}^z/N, \qquad (3)$$

where $\langle\cdots\rangle$ represents an average first over Monte Carlo timestep for each sample and then over samples of different random distributions, and the relation, $\chi_{\rm SG} = N\langle q_{\alpha\beta}\rangle^2$, holds. The glass transition T_c is determined by the binder analysis, and the finite size scaling analysis on $\chi_{\rm QSG} = L^{2-\eta}\tilde{\chi}((T - Tc)L^{1/\nu})$ demonstrates the existence of the spin glass phase[2]. However, whether there exists a finite temperature spin glass phase had been the subject of intense controversy from the 1970s. We partially follow this standard analysis, while finding after all that our spin glass cannot be simply understood within the numerical framework which worked to detect the conventional spin glass.

We performed the continuous imaginary time quantum Monte Carlo calculation to the $L\times L$ lattices with $L = 36, 48, 60$. We find that there occurs a Berezinskii-Kosterlitz-Thouless (BKT) transition at around $k_BT_{\rm BKT}/J = 0.2-0.4$. Below that temperature, the antiferromagnetic correlation develops, and the introduction of the randomness gives rise to the spin glass transition at $k_BT_{\rm sg}/J \sim 0.05 - 0.1$. The transition is detected by the Replica symmetry breaking(RSB); the L dependent behavior of the replica overlap distribution $P(q)$ shows the emergent peaks at both $q = 0$ and $q \neq 0$ indicating the two-step RSB.

By further analyzing the $\chi_{\rm SG}$, we found a particular peak structure developing at around $T_{\rm sg}$. This peak sustains even after subtracting the classical $\chi_{\rm SG}$ we obtained parallelly by setting $\Gamma = 0$. We thus consider that there is a quantum mechanical contribution to $\chi_{\rm SG}$ particular to this model. Our spin glass phase protected by the BKT phase, and disappears together with the BKT phase for $R > 0.15 - 0.2$. The work is in collaboration with Kazumasa Ueda and Masatoshi Imada in preparation.

References

[1] L. Binder and A. P. Young: Rev. Mod. Phys. **58** (1986).

[2] N. Kawashima and A. P. Young: Phys. Rev. B **53** (1996) R484 .

Photoinduced nonequilibrium dynamics in correlated electron systems

Sumio Ishihara
Department of Physics, Tohoku University

Opto-spintronics in correlated magnets

Ultrafast optical control of magnetism has attracted much interest in the recent years, accompanied by rapid progress in laser light technologies. We analyze the double exchange (DE) model defined by

$$H = \sum_{ijs} h_{ij} c_{is}^{\dagger} c_{js} - \frac{J}{S} \sum_{iss'} S_i \cdot \sigma_{ss'} c_{is}^{\dagger} c_{is'}, \quad (1)$$

where $c_{is}^{\dagger}(c_{is})$ is a creation (annihilation) operator of a conduction electron with spin s $(= \uparrow, \downarrow)$ at site i, S_i is a localized-spin operator with magnitude S, and σ^{α} $(\alpha = x, y, z)$ are the Pauli matrices. The first term represents the hopping of the conduction electrons with the transfer integral h_{ij}, and the second term represents the Hund coupling between the conduction electrons and the localized spins with the coupling constant J (> 0). It was shown that an initial ferromagnetic (FM) metal state is changed to an almost perfect antiferromagnetic (AFM) state by photoirradiation [1], which is in sharp contrast to the naive DE scenario in equilibrium states. In this theme, we study furthermore this issue.

1) In order to elucidate the microscopic mechanism that drives the FM state into the AFM state, we study the magnetic structure in a cw field by using the Floquet Green function [2]. We show that a magnon dispersion is softened and forms a dip at momentum $q = (\pi, \pi)$ by the photoirradiation, which indicates that the AFM instability develops at finite threshold intensity. An nonequilibrium electron distribution plays an essential role to induce the instability. We show that an interband-excitation peak and Floquet side peaks appear in the transient and steady states.

2) We study the topological spin textures in the photoinduced nonequilibrium state in a metallic magnetic system [3]. We focus on the transient spin structure described by the DE model from the initial FM state to the AFM ordered state. We find emergence of the topological spin texture in the photoinduced transient state through the calculation of the real-space spin configuration, the Pontryagin index, and the scalar chirality. This observation is reproduced by analyzing the thermalization spin dynamics after chemical-potential quench in a large cluster.

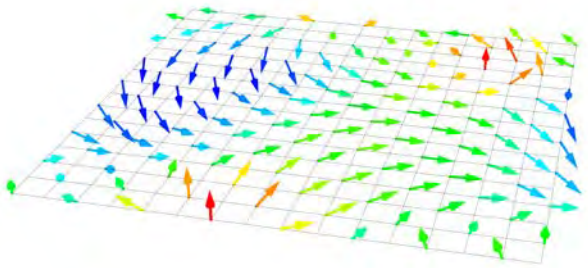

Figure 1: Snapshots of the localized spin configurations in a sublattice [3].

Complexed quantum dynamics in strongly interacting systems

Excitonic insulator (EI) has been proposed more than a half century ago in semiconductors and semimetals, has been studied intensively in the theoretical and experimental sides. When the attractive Coulomb inter-

action between electrons and holes overcomes the gap energy, the electron-hole pairs, i.e. excitons, are produced spontaneously to gain the system energy. Owing to the recent great progresses of the experimental technique, the study of the EI state is revived. Some examples materials are 1T-$TiSe_2$ and $TaNiSe_5$. A major problem of the research subjects is how to identify the EI state and transition. A new direct route to identify the EI state in experiments is required to progress this research field.

In this theme, we study the optical responses in EI states [4]. We adopt the two-orbital Hubbard model with finite energy difference between the orbitals defined by

$$\begin{aligned} H &= \Delta \sum_{i\sigma}(n_{ia\sigma} - n_{ib\sigma}) + \sum_{\langle ij\rangle\alpha\sigma} t_\alpha c^\dagger_{i\alpha\sigma} c_{j\alpha\sigma} \\ &+ \sum_i (U \sum_\alpha n_{i\alpha\uparrow} n_{i\alpha\downarrow} + U' n_{ia} n_{ib}) \\ &+ J \sum_{i\sigma\sigma'} c^\dagger_{ia\sigma} c^\dagger_{ib\sigma'} c_{ia\sigma'} c_{ib\sigma} \\ &+ I \sum_{i\alpha} c^\dagger_{i\alpha\uparrow} c^\dagger_{i\alpha\downarrow} c_{i\bar{\alpha}\downarrow} c_{i\bar{\alpha}\uparrow}, \end{aligned} \tag{2}$$

where $c_{i\alpha\sigma}$ is an annihilation operator of an electron with spin $\sigma(=\uparrow,\downarrow)$ and the orbital $\alpha(=a,b)$ at site i, and $n_{i\alpha\sigma} = c^\dagger_{i\alpha\sigma} c_{i\alpha\sigma}$ is the particle number operator. This model is analyzed by utilizing the variational cluster approach. The optical conductivity spectra are formulated in the two-particle Greens function, in which the vertex corrections are taken into account. The finite temperature phase diagram and the one-particle excitation spectra are obtained by considering the EI phase, the high-spin(HS) AFM phase and the low-spin (LS) and HS (HS/LS) ordered phase.

A unique peak structure appears in the EI state, energy of which is of the order of the intra-site inter-obital Coulomb interaction. This is due to the hybridization between the two orbitals, which is opened in the EI phase. The peak intensity almost follows the EI order parameter as shown in Fig. 2. We propose that this peak is available to identify the EI state.

These researches have been performed with collaboration with A. Ono, H. Li, M. Naka and J. Ohtsuki. The numerical calculations in these works have been done using the facilities of the Supercomputer Center, the Institute for Solid State Physics, the University of Tokyo.

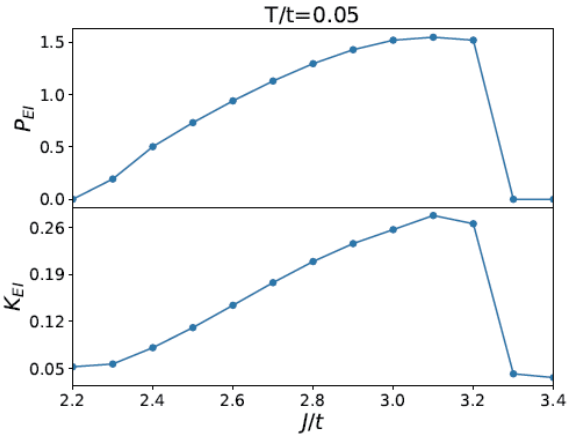

Figure 2: EI peak intensity and the EI order parameters as function of the Hund coupling parameter [4].

References

[1] A. Ono and S. Ishihara: Phys. Rev. Lett. **119**, 207202 (2017).

[2] A. Ono and S. Ishihara: Phys. Rev. B **98**, 214408 (2018).

[3] A. Ono, S. Ishihara: J. Phys. Soc. Jpn. **88**, 023703 (2019) .

[4] H. Li, J. Otsuki, M. Naka and S. Ishihara (unpublished).

Optimization variational Monte Carlo study of strongly correlated electron systems

Takashi YANAGISAWA
Electronics and Photonics Research Institute
National Institute of Advanced Industrial Science and Technology (AIST)
AIST Central 2, 1-1-1 Umezono, Tsukuba 305-8568

We have investigated the ground-state properties of the two-dimensional Hubbard model and the d-p model by using the optimized variational Monte Carlo method[1, 3, 4]. We performed parallel computation in Monte Carlo calculations. In order to reduce statistical errors, we carried out 100 $\sim$ 200 parallel calculations. Parallel computing is very helpful to reduce Monte Carlo statistical errors.

We used the wave function of an $\exp(-\lambda K) - P_G$-type wave function. This wave function is very excellent in the sense that the ground-state energy is lowered greatly and the ground-state energy is lower than that evaluated by any other wave functions[3]. We can improve the wave function systematically by multiplying by operators P_G and $e^{-\lambda K}$ many times.

We show the condensation energy as a function of the hole doping rate x in Fig. 1[4]. The calculations were performed on a 10×10 lattice with $U/t = 18$ and $t' = 0$. There are three phases: the antiferromagnetic insulator state (AFI), the coexistent state of antiferromagnetism and superconductivity (AF+SC) and the d-wave superconducting state (SC). Near half-filling for approximately $0 \leq x < 0.06$, the ground state is an AF insulator. The coexistent state exists for $0.06 < x < 0.09$. When the doping rate is as large as $x > 0.09$, the ground state is d-wave superconducting state. High-temperature superconductivity will occur in the SC phase in this figure. The reason why the AFI phase exists near $x = 0$ is due to the instability toward the phase separation. In the phase-separated state, the doped holes are not conductive.

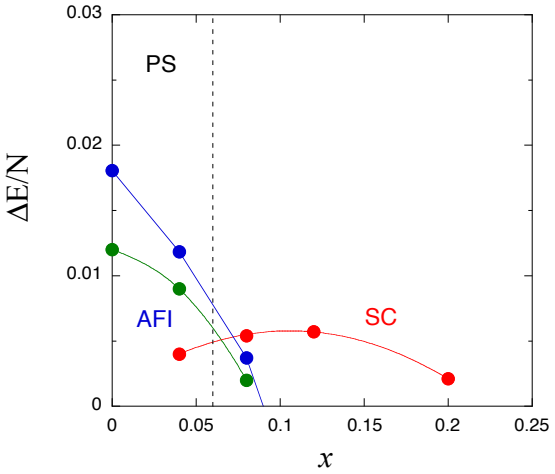

Figure 1: The condensation energy per site as a function of the hole density $x = 1 - n_e$ on a 10×10 lattice, where the wave function is $\psi_\lambda = \psi^{(2)}$. We set $t' = 0$ and $U/t = 18$. We used the wave function $\psi^{(4)}$ for the lower AF curve. In the region where $x \leq 0.06$, the ground state is an insulator due to the instability toward the phase separation.

References

[1] T. Yanagisawa et al., J. Phys. Soc. Jpn. 67, 3867 (1998).

[2] T. Yanagisawa, Phys. Rev. B75, 224503 (2007) (arXiv: 0707.1929).

[3] T. Yanagisawa, J. Phys. Soc. Jpn. 85, 114707 (2016).

[4] T. Yanagisawa, J. Phys. Soc. Jpn. 88, 054702 (2019).

Drawing phase diagram from many-variable variational wave functions with machine learning

Yuichi Motoyama
Institute for Solid State Physics, University of Tokyo
Kashiwa-no-ha, Kashiwa, Chiba 277-8581

Recently, machine learning (ML) techniques are applied for drawing a phase diagram, because this is a kind of classification problems or clustering problems, where machine learning techniques are widely used. For example [1], a well trained model (e.g., a neural network) can tell whether a spin configuration of the Ising model is generated from the ferromagnetic phase (the ordered phase) or the paramegnetic phase (the disordered phase.) For another example [2], performing the principal components analysis method, in other words, the singular value decomposition of spin configurations can detect the phase transition point. The former is an example of a supervised training and the latter is an example of an unsupervised training. For the both cases, no specific order parameters such as the spontaneous magnetization are explicitly supposed, but the machine learning models automatically extract some features to represent each phase. In the ML methods, therefore, we become free from finding the order parameter. Unfortunately, another problem appears – how to choose the input of the ML model. For the classical spin systems such as the Ising model, several studies have shown that a spin configuration can be used as an input of a ML model. It should be noted that for some models the way to represent a spin configuration is not unique, and the accuracy of the ML model sometimes depends on the representation. The XY model, for example, the state of one spin, a vector $\vec{\sigma}$, can be represented by the angle θ between $\vec{sigma}$ and the x axis or the components of $\vec{\sigma}$, say, $(\cos\theta, \sin\theta)$. In the present author's experience, the latter representation seems to be better than the former. For strongly correlated systems, on the other hand, the general input has not yet appeared. One of reasons is that there are no methods for obtaining the ground state of an arbitrary system, in other words, each method has own advantages and disadvantages.

In this study, we tried to generate inputs of ML models by using the variational Monte Carlo (VMC) method [3, 4]. The VMC method is one of the powerful methods for obtaining the ground state of strongly correlated systems, which can deal with larger system than the exact diagnonalization method and is free from the infamous sign problem breaking the path-integral Monte Carlo method down. In the VMC method, we prepare some form of the wavefunction $|\psi(\alpha)\rangle$ with some parameters α, which is called as a variational wavefunction or a trial wavefunction. From the variational principle, we can find the wavefunction of the ground state by tuning α to minimize the energy of the wavefunction $|\psi(\alpha)\rangle$. The expectation value of an arbitrary physical quantity A with respect to $|\psi\rangle$ is rigorously written as the following;

$$\begin{aligned}\langle A\rangle_\psi &= \frac{\langle\psi|A|\psi\rangle}{\langle\psi|\psi\rangle} = \frac{\sum_x \langle\psi|x\rangle\langle x|A|\psi\rangle}{\langle\psi|\psi\rangle} \\ &= \sum_x \frac{|\langle\psi|x\rangle|^2}{\langle\psi|\psi\rangle}\frac{\langle x|A|\psi\rangle}{\langle x|\psi\rangle}\end{aligned} \tag{1}$$

where $|x\rangle$ is some handy wavefunction which

forms a complete system. In the VMC method, we perform the Markov chain Monte Carlo method for generating $|x\rangle$ with the weight function $\rho(x) \equiv |\langle\psi|x\rangle|^2 \,/\, \langle\psi|\psi\rangle$ in order to take the summation over x. For quantum lattice models such as the Fermion-Hubbard model and the Heisenberg model, we can adopt the Fock states of electrons for $|x\rangle$. In this study, we investigated whether $|x\rangle$ can be used as an input of ML model or not by using the transverse field Ising chain as demonstration. $|x\rangle$ plays the same role as that of spin configurations in the classical systems where a configuration x appears with the probability $p(x) = \exp(-\beta E(x))$. This corresponding is an advantage of our choice. We modified and used a program package implementing the many-variables VMC, `mVMC` [4, 5].

References

[1] J. Carrasquilla and R. G. Melko, nat. phys. **13**, 431 (2017).

[2] L. Wang, Phys. Rev. B **94**, 195105 (2016).

[3] C. Gros, Ann. Phys. **189**, 53 (1989).

[4] T. Misawa, *et al.*, Comp. Phys. Comm. **235**, 447 (2019).

[5] `https://github.com/issp-center-dev/mVMC`.

Two competing superconducing phases in κ-type molecular conductors

Hiroshi WATANABE
Waseda Institute for Advanced Study, Waseda University
1-6-1 Nishi Waseda, Shinjuku-ku, Tokyo 169-8050

The family of quasi two-dimensional molecular conductors κ-(BEDT-TTF)$_2$X has been extensively studied as a typical example of strongly correlated electron system. Depending on the monovalent anion X, they show various quantum phases such as antiferromagnetic and spin-liquid dimer-Mott insulators, and superconductivity (SC) [1]. Owing to the similarities in the experimental phase diagrams, κ-(BEDT-TTF)$_2$X system is often compared with high-T_c cuprates, which exhibit Mott metal-insulator transition and SC [2]. Recently, carrier doping in κ-(BEDT-TTF)$_2$X has been realized using electric-double-layer transistor [3], and the direct comparison with cuprates becomes possible. The experimental result shows the electron-hole doping asymmetry, reminiscent of the high-T_c cuprates.

Here, we theoretically study the doping effect in κ-(BEDT-TTF)$_2$X [4]. We consider a four-band extended Hubbard model including onsite (U) and intersite Coulomb interactions (V_{ij}) with κ-type geometry with the largest hopping integral t_{b_1} as an energy unit. The ground state properties are studied with the variational Monte Carlo (VMC) method. The Gutzwiller-Jastrow type wave function is used for the VMC trial wave function. The system sizes for calculation are from 288 (2×12×12) to 1152 (2×24×24).

In the ground-state phase diagram, there appear various competing phases and a significant electron-hole doping asymmetry is observed [4]. Here, we focus on the change of the most favored gap symmetry of SC. Figure 1 shows the ground-state phase diagram in a $n_{\rm hole}$-U/t_{b_1} space. Only the SC phases are considered and other ordered phases are ignored. The largest intersite Coulomb interaction is fixed at V_{b_1}/U=0.5. For the hole-doped side, the d_{xy}-wave symmetry, which has similarities with high-T_c cuprates, is favored. On the other hand, for the undoped and electron-doped side, the extended-s+$d_{x^2-y^2}$-wave symmetry [5, 6, 7] is favored. The change of the symmetry of SC is attributed to the degree of frustration that is controlled by carrier doping. This is a new perspective to κ-(BEDT-TTF)$_2$X, which can also be applied to other frustrated systems in general.

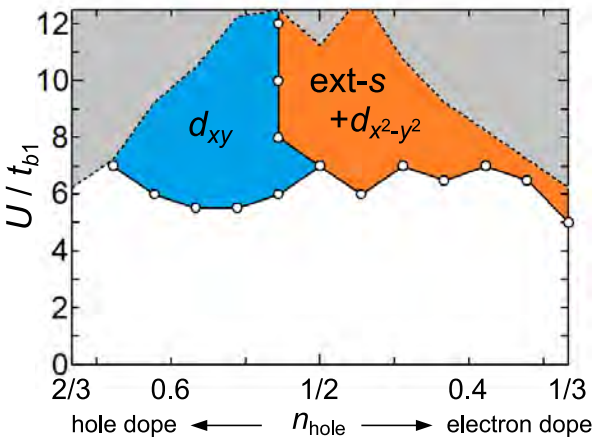

Figure 1: Ground-state phase diagram of the extended Hubbard model for κ-(BEDT-TTF)$_2$X. Only the superconducting phases are considered.

References

[1] K. Kanoda: J. Phys. Soc. Jpn. **75** (2006) 051007.

[2] R. H. McKenzie: Science **278** (1997) 820.

[3] Y. Kawasugi et al., Nat. Commun. **7** (2016) 12356.

[4] H. Watanabe, H. Seo, and S. Yunoki: submitted, arXiv: 1811.09035.

[5] K. Kuroki, T. Kimura, R. Arita, Y. Tanaka, and Y. Matsuda: Phys. Rev. B **65** (2002) 100516(R).

[6] D. Guterding, M. Altmeyer, H. O. Jeschke, and R. Valentí, Phys. Rev. B **94** (2016) 024515.

[7] H. Watanabe, H. Seo, and S. Yunoki: J. Phys. Soc. Jpn. **86** (2017) 033703.